Article

Chinese Science Bulletin

Atomic & Molecular Physics

December 2012 Vol.57 No.36: 4712–4717
doi: 10.1007/s11434-012-5569-1

Theoretical study on stereodynamics of H + NeH^+ ($v = 0, j = 0$) → H_2^+ + Ne reaction

YIN ShuHui[1*], ZOU JingHan[1], GUO MingXing[2], XU XueSong[1], GAO Hong[1], LI Lei[1] & CHE Li[1]

[1] *Department of Physics, Dalian Maritime University, Dalian 116026, China;*
[2] *Environmental Science and Engineering College, Dalian Maritime University, Dalian 116026, China*

Received April 29, 2012; accepted July 16, 2012

Stereodynamics of reaction H + NeH^+ ($v = 0, j = 0$) → H_2^+ + Ne is investigated by quasi-classical trajectory method using a new potential energy surface constructed by Lv et al. The distributions of $P(\theta_r)$, $P(\phi_r)$ and PDDCSs are calculated at four different collision energies. The rotational polarization of product H_2^+ presents different characters at different collision energies. The product rotational angular momentum vector $\boldsymbol{j'}$ is not only aligned, but also oriented along the direction perpendicular to the scattering plane. With the increase of collision energy, the rotation of product molecule has a preference of changing from the "in-plane" mechanism to the "out-of-plane" mechanism. Although the title reaction is mainly dominated by the direct reaction mechanism, the indirect mechanism plays a role when the collision energies are low.

reaction stereodynamics, quasi-classical trajectory, polarization, alignment

Citation: Yin S H, Zou J H, Guo M X, et al. Theoretical study on stereodynamics of H + NeH^+ ($v = 0, j = 0$) → H_2^+ + Ne reaction. Chin Sci Bull, 2012, 57: 4712–4717, doi: 10.1007/s11434-012-5569-1

Chemical reactions have been studied mainly by the measurements and calculations of scalar properties such as rate constant, cross section and product population distributions. However, complete information on the forces acting in the reaction also requires a consideration of vector properties, as they are key indicators of the anisotropy of the potential energy surface involved in the reaction [1–7]. Herschbach and co-workers have undertaken some pioneering works on the dynamical stereochemistry [8–11]. Vector properties, such as velocities and angular momentum, possess not only magnitudes that can be directly related to translational and rotational energies, but also well-defined directions.

In the past three decades, the endothermic atom-molecule ion reaction Ne + H_2^+ → NeH^+ + H has been widely studied in high-quality experiments and theoretical dynamics simulations. Bilotta et al. [12] provided angular distributions and flux contour maps according to the results of a crossed molecular beam experiment. Van Pijkeren et al. [13] measured the relative energy-dependent cross sections for H_2^+ ($v = 0$–8) using the photoelectron-secondary ion coincidence (PESICO) technique. In a threshold electron-secondary-ion-coincidence (TESICO) experiment, Herman et al. [14] investigated the relative cross sections for $v = 0$–4 as a function of translational energies. A recent experimental work [15] reported the absolute cross sections involving an initial rotational state $j = 1$ and vibrational states $v = 0$–17 for collision energy 0.7 eV, $v = 0$–14 for 1.7 eV and $v = 0$–12 for 4.5 eV, respectively. Theoretically, Kress et al. [16] reported the state to state reaction probabilities using an approximate quantum dynamics calculation. Gilibert and co-workers [17,18] presented the state-selected integral cross sections using the coupled-states approximation (CSA). Recently, Mayneris-Perxachs et al. [19] carried out a time-dependent quantum dynamics study at the centrifugal sudden level (CS-RWP method) to investigate the influence of vibrational excitation of H_2^+ ($v = 0$–9, $j = 0$) and D_2^+ ($v =$

*Corresponding author (email: yinsh@dlmu.edu.cn)

0–12, $j = 0$). These studies were almost based on the analytical potential energy surface (PES) constructed by Pendergast et al. (PHHJ3) [20]. In 2010, Lü et al. [21] (LZHH) reported a new PES that was fitted from 7000 energy points. The LZHH PES agrees fairly well with experimental results over the collision energy range under 2.8 eV. Based on the LZHH PES, Xiao et al. [22] discussed vector correlation between reagents and products at different collision energies using quasi-classical trajectory (QCT) method. The isotopic effects on the stereodynamics of Ne + H_2^+/Ne + HD^+/Ne + HT^+ were also studied using QCT method [23] on the same LZHH PES. These results showed a perfect agreement with the experimental results, which further demonstrates that the LZHH PES is accurate and useful for dynamical calculation.

Most of the studies have focused on the reaction Ne + H_2^+ and its isotopic effect; yet the reverse reaction H + NeH^+ has seldom been studied to date. To shed more light on this reverse reaction, in this paper we will adopt a QCT calculation on the new LZHH PES.

1 Theory

In the present calculations, we use the new 3D adiabatic PES constructed by Lv et al. The PES was computed using complete active space self-consistent field (CASSCF) and internally contracted multireference configuration interaction (MRCI) wave function with aug-cc-pv5z basis set. In both CASSCF and MRCI calculations, nine valence electrons were included in ten active orbitals (8a′+2a″), consisting of H 1s orbitals and the 2s, 2p, 3s and 3p orbitals of the Ne atom. The remaining orbital was kept doubly occupied. In the calculation, equal weights were assigned to each of the three states ($1^2A'$, $2^2A''$, $1^2A''$) in the state-averaging calculations. In addition, the multireference Davison correction [24] (+Q) was included to compensate for the effect of higher order correlation. The analytical representation of the PES was fitted with 7026 *ab initio* energies below 2.8 eV relative to the dissociation energy of Ne + H_2^+. The analytical expression of the PES was represented by the Aguado-Paniagua function [25]. Compared to the *ab initio* data, the rms error was 0.27 kcal/mol and the maximum energy deviation was 2.7 kcal/mol, which is more accurate than previous PES [20]. The cross sections ($v = 0$, $j = 1$) with Coriolis coupling effect based on the new PES are found to be in good agreement with the available experimental data [15]. Only a deep well at the collinear configuration on the LZHH PES, with no other wells or barriers were found for this configuration. The depth of well becomes shallower and a barrier appears with the decrease of Ne-H-H angle.

The full three-dimensional angular distribution related $\boldsymbol{k}$-$\boldsymbol{k}'$-$\boldsymbol{j}'$ can be represented by a set of generalized PDDCSs in the center-of mass (CM) frame. The reagent relative velocity vector $\boldsymbol{k}$ is parallel to the z-axis, and the x-z plane is the scattering plane containing the initial and final relative velocity vectors, $\boldsymbol{k}$ and $\boldsymbol{k}'$. The angle θ_t is the so-called scattering angle between the reagent relative velocity and the product relative velocity. θ_r and ϕ_r are the polar and azimuthal angles of the final rotational angular momentum $\boldsymbol{j}'$. The standard QCT method (see the details in [26–29] and the references therein) is employed to study the stereodynamics of the title reaction. The classical Hamilton's equations are numerically integrated in three dimensions. Considering the well at collinear geometry with the depth about 12.5 kcal/mol on the LZHH PES with respect to the reaction asymptote, several collision energies lower than well depth were chosen to explore the well effect on the title reaction. Four collision energies (0.5, 2, 8, 20 kcal/mol) were chosen for the title reaction. The vibrational and rotational levels of NeH^+ were taken as $v = 0$ and $j = 0$, respectively. In this calculation, batches of 100000 trajectories were run for each reaction and integration step size is chosen as 0.1 fs. The trajectories were started at an initial distance of 10 Å between the H atom and the centre of the mass of the NeH^+ molecule.

2 Results and discussion

The $P(\theta_r)$ distributions of the product H_2^+, describing the $\boldsymbol{k}$-$\boldsymbol{j}'$ correlation, are shown in Figure 1. From Figure 1, the $P(\theta_r)$ distributions peak at θ_r angles close to 90° and are symmetric with respect to 90°, which demonstrates that the product rotational angular momentum vector $\boldsymbol{j}'$ is distributed with cylindrical symmetry in the product scattering frame, and the direction of $\boldsymbol{j}'$ is preferentially aligned perpendicular to $\boldsymbol{k}$ direction. The peak of $P(\theta_r)$ becomes broader and lower as the collision energy increases from 0.5 to 8 kcal/mol, indicating that the product rotational alignment becomes weaker with the increase of the collision energy. It is interesting that the peak of $P(\theta_r)$ becomes higher and narrower as the collision energy increases to 20 kcal/mol, which

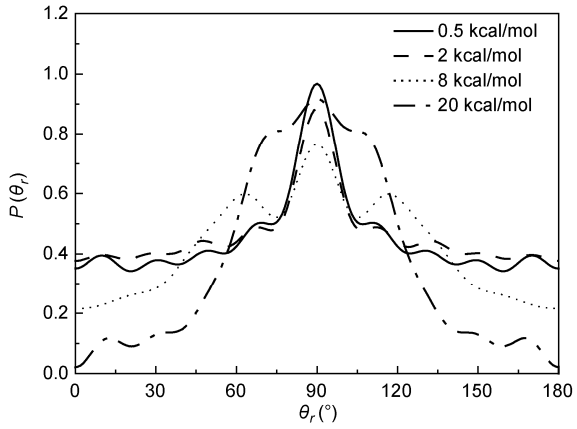

Figure 1 Angular distribution of $P(\theta_r)$, reflecting the $\boldsymbol{k}$-$\boldsymbol{j}'$ correlation, at E_{col} = 0.5, 2, 8 and 20 kcal/mol.

means the degree of rotational alignment of the product has an increasing trend as the collision energies continue to increase. This trend is confirmed by the values of the product average rotational alignment parameter $\langle P_2(\boldsymbol{j}'\cdot\boldsymbol{k})\rangle$, as shown in Figure 2. From Figure 2, the value of $\langle P_2(\boldsymbol{j}'\cdot\boldsymbol{k})\rangle$ increases first and then decreases rapidly with the increase of collision energy. The tendency of $\langle P_2(\boldsymbol{j}'\cdot\boldsymbol{k})\rangle$ indicates that the degree of product rotational alignment decreases at first and then increases with the increase of collision energy (the smaller the value of $\langle P_2(\boldsymbol{j}'\cdot\boldsymbol{k})\rangle$, the stronger the alignment of product). This trend of $\langle P_2(\boldsymbol{j}'\cdot\boldsymbol{k})\rangle$ is consistent with the result of $P(\theta_r)$. According to important research by Han et al. [30], who reported the product rotational polarization of "A + BC" reactions with different reagent mass combinations on different potential energy surfaces, the rotational alignments of products are sensitive to two factors: one is the characters of the PES, and the other is the mass factor. The tendency of $\langle P_2(\boldsymbol{j}'\cdot\boldsymbol{k})\rangle$ for the title reactions is in accordance with attractive PESs, which implies that the exoergic process of the title reaction takes place on the entrance valley of the PES. The decrease of product rotational alignment with the increase of collision energy from 0.5 to 8 kcal/mol can be attributed to the well on the PES. When the collision energy is low, some trajectories will be "trapped" in the well. The existence of well on PES lead complex to have longer lifetime to make angular momentum lose memory of initial direction [31,32]. As a result, the product rotational polarization is weak at low collision energies. However, when the collision energy is high enough, the product H_2^+ with higher internal energy can move with less effort away from the well. Therefore the degree of product alignment shows augment with the increase of collision energy.

The dihedral angle distributions of $P(\phi_r)$ shown in Figure 3, describe the $\boldsymbol{k}$-$\boldsymbol{k}'$-$\boldsymbol{j}'$ correlations. From Figure 3, the $P(\phi_r)$ distributions are asymmetric with respect to the $\boldsymbol{k}$-$\boldsymbol{k}'$ scattering plane (or about ϕ_r = 180°), directly reflecting the strong polarization of product rotational angular momentum. The peaks of $P(\phi_r)$ appear at ϕ_r = 90° and 270°, which

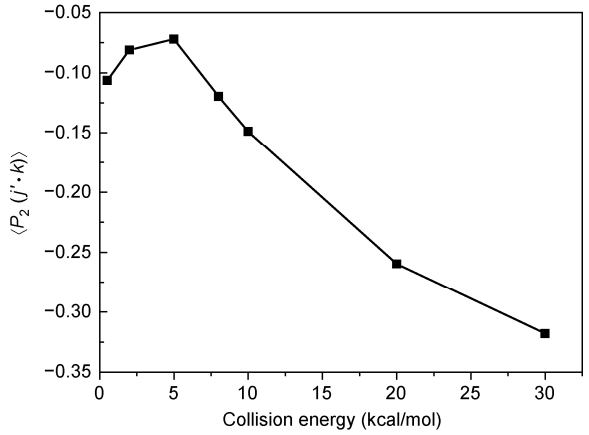

Figure 2 Product rotational alignment parameter $\langle P_2(\boldsymbol{j}'\cdot\boldsymbol{k})\rangle$ as a function of collision energy.

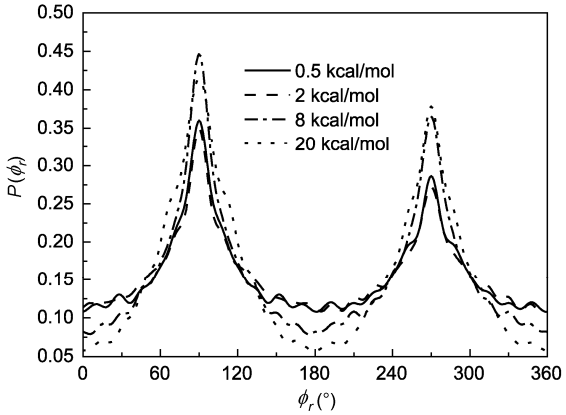

Figure 3 Dihedral angle distribution of $\boldsymbol{j}'$, $P(\phi_r)$, with respect to the $\boldsymbol{k}$-$\boldsymbol{k}'$ plane, for product H_2^+ from H + NeH^+ (v = 0, j = 0) → H_2^+ + Ne at E_{col} = 0.5, 2, 8 and 20 kcal/mol.

shows that the rotational angular momentum vector of product H_2^+ is mainly aligned along y-axis of CM frame. As the peak at ϕ_r = 90° is not equal to that at ϕ_r = 270° for a fixed collision energy, the product rotational angular momentum vector $\boldsymbol{j}'$ is not only aligned, but also oriented along the y-axis. The peak at ϕ_r = 90° is slightly higher than that at ϕ_r = 270° for four collision energies, which means the $\boldsymbol{j}'$ is preferentially oriented along the positive direction of y-axis. We will use the term "in-plane" to refer to the preference of product molecule rotating in planes parallel to the scattering plane, whereas the term "out-of-plane" to refer to the preference of product molecule rotating in the planes perpendicular to the scattering plane. The peaks at higher collision energies are broader showing that the product molecule rotation has a preference of changing from "in-plane" reaction mechanism to the "out-of-plane" mechanism. A similar phenomenon was also found in the reactions of H′ + HBr, H + LiH^+, H + HeH^+ [33–35]. In the title reaction, the distribution of $P(\theta_r)$ is symmetric, while the distribution of $P(\phi_r)$ is asymmetric. The probable reason may be the repulsive energy between Ne-H^+ atoms, leading to the violation of the symmetry when the reaction occurs. The behavior can be understood by the "Impulsive-Collision Model" [36,37] of the atom-molecule reaction developed by Han et al. In reaction A + BC → AB + C, the product rotational angular momentum $\boldsymbol{j}'$ can be expressed as $\boldsymbol{j}' = \boldsymbol{L}\sin^2\beta + \boldsymbol{j}\cos^2\beta + \boldsymbol{J}_1 m_B/m_{AB}$, where $\boldsymbol{L}$ and $\boldsymbol{j}$ are the orbital and rotational angular momentum of the reactant molecule AB, respectively. $\boldsymbol{J}_1 = \sqrt{\mu_{BC}R}\,(\boldsymbol{r}_{AB} \times \boldsymbol{r}_{CB})$, with $\boldsymbol{r}_{AB}$ and $\boldsymbol{r}_{CB}$ being unit vectors where B pointing to A and C, respectively. The μ_{BC} is the reduced mass of the BC molecule and R is the repulsive energy between B and C atoms. During the chemical bond forming and breaking for the title reaction, the term $\boldsymbol{L}\sin^2\beta + \boldsymbol{j}\cos^2\beta$ in the equation is symmetric with respect to the $\boldsymbol{k}$-$\boldsymbol{k}'$ scattering plane, whereas the term $\boldsymbol{J}_1 m_B/m_{AB}$ has a preferred direction because of the effect of the repulsive energy

R, which causes the orientation of the products H_2^+.

The generalized polarization-dependent differential cross sections (PDDCSs) can give a description of the $\boldsymbol{k}$-$\boldsymbol{k'}$-$\boldsymbol{j'}$ correlation and the scattering direction of the product molecule, which are plotted in Figure 4. The PDDCS $(2\pi/\sigma)(\mathrm{d}\sigma_{00}/\mathrm{d}\omega_t)$, which is simply the differential cross-section (DCS), only describes the $\boldsymbol{k}$-$\boldsymbol{k'}$ correlation or the scattering direction of the product and is not associated with the orientation and alignment of the product rotational angular momentum vector $\boldsymbol{j'}$. The scattering direction of the product H_2^+ is related to the collision energies. As shown in Figure 4(a), the product H_2^+ are mainly forward scattering at the four collision energies. Over the collision energy range of 0.5–20 kcal/mol, with the increase of collision energy, the tendency of forward scattering increases quickly. To pursue the reason for this interesting phenomenon, the variation of internuclear distances of H-Ne, H^+-Ne and H-H^+ are presented as a function of propagation time in Figure 5. According to the DCSs, the trajectories are selected in the scattering angle ranges of θ_t= 0°–30° and 150°–180° at E_{col} = 0.5 kcal/mol and 0°–30° at both E_{col} = 2 kcal/mol and E_{col} = 20 kcal/mol. From Figure 5(a) and (b), attacking atom H collides with target molecule NeH^+ and forms an H_2^+ product that moves away immediately. This process is consistent with direct reactive mechanism. As shown in Figure 5(c) and (d), we find indirect reactive trajectories, namely "trapped" trajectories. From Figure 5(c) and (d), it is apparently that atom H suffers more than one collision with NeH^+ and the complexes have relatively long lifetimes before forming the product H_2^+. The long-time survival enables the system to perform abundant rotations before breaking up into one possible channel, so the products have more random directions. However, at higher collision energies, we rarely find indirect reactive trajectories. That may the reason that the tendency of backward scattering of H_2^+ are stronger at lower collision energies. As mentioned above, the LZHH PES is attractive, together with LHL mass combination characteristics of the title reaction, we can infer that the product molecules are forward scattering with direct reaction mechanism [30]. As shown in Figure 4(a), the forward scattering is still stronger than backward at low collision energies although indirect trajectories exist at low collision energies. Therefore, direct reaction mechanism is dominant even at low collision energy. Therefore, we can reach a conclusion that the title reaction is mainly governed by the direct reaction mechanism, and the indirect reactive play a role when the collision energies are low. This observation is consistent with the distribution of $\langle P_2(\boldsymbol{j'}\cdot\boldsymbol{k})\rangle$ shown in Figure 2. The value of $\langle P_2(\boldsymbol{j'}\cdot\boldsymbol{k})\rangle$ has a slight increase when collision energy under 5 kcal/mol, indicating the degree of product polarization is weak at low collision energies.

The PDDCS $(2\pi/\sigma)(\mathrm{d}\sigma_{20}/\mathrm{d}\omega_t)$ is the expectation value of the second Legendre moment $\langle P_2(\cos\theta_r)\rangle$, which is shown in Figure 4(b). The behavior of $(2\pi/\sigma)(\mathrm{d}\sigma_{20}/\mathrm{d}\omega_t)$ demonstrates that the trend is opposite to that of $(2\pi/\sigma)(\mathrm{d}\sigma_{00}/\mathrm{d}\omega_t)$, indicating that $\boldsymbol{j'}$ is strongly aligned perpendicular to $\boldsymbol{k}$. From Figure 4(b), $\boldsymbol{j'}$ is preferentially polarized along the direction perpendicular to $\boldsymbol{k}$ at θ_t = 0°. As illustrated in Figure 4(c)

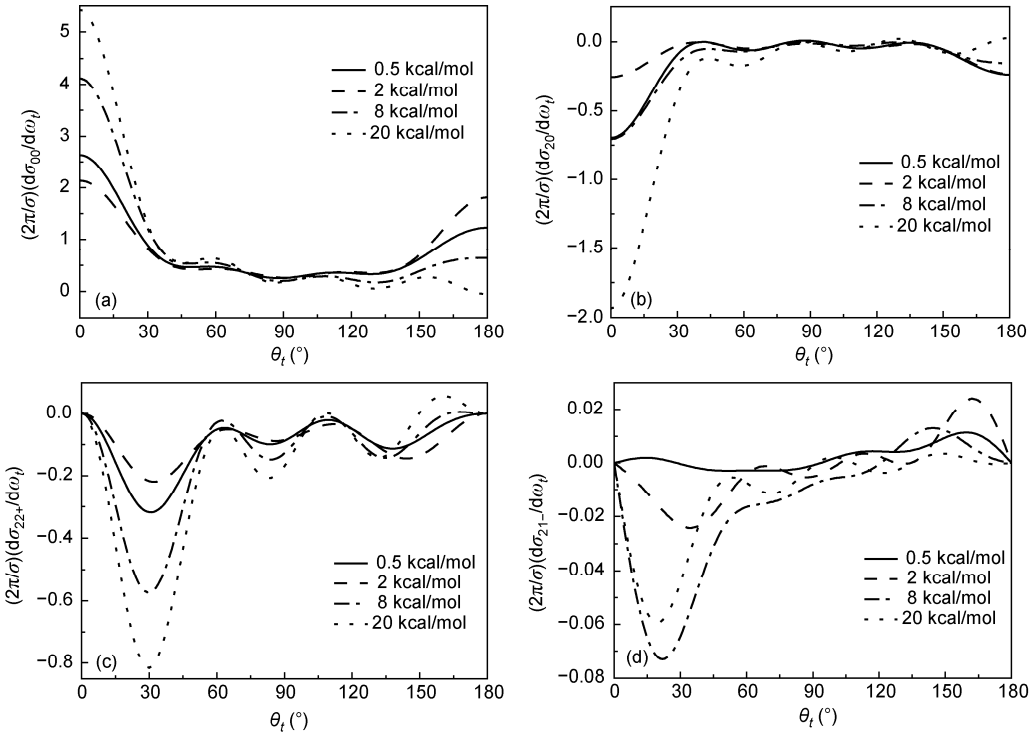

Figure 4 PDDCSs of H + NeH^+ ($v = 0, j = 0$) → H_2^+ + Ne at E_{col} = 0.5, 2, 8 and 20 kcal/mol.

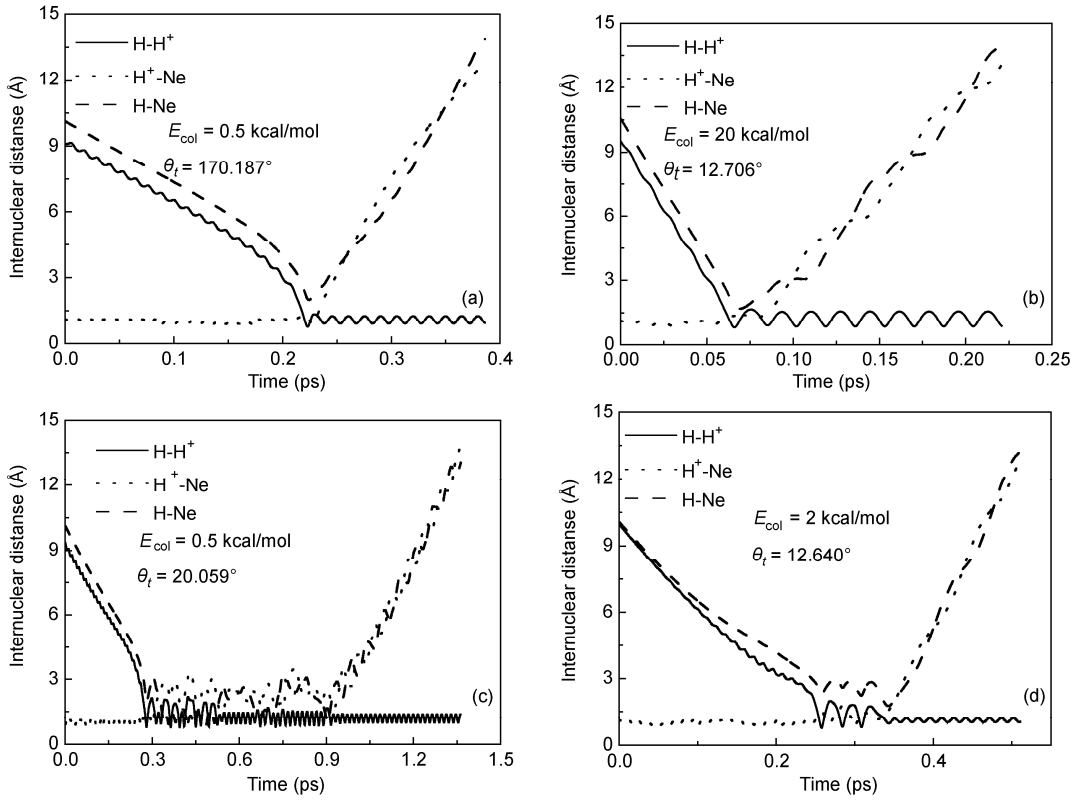

Figure 5 Internuclear distance of H-Ne, H^+-Ne and H-H^+ as a function of propagation time.

and (d), the PDDCSs with $q \neq 0$ are equal to zero at the extremities of forward and backward scattering. At these limited scattering angles, the $\boldsymbol{k}$-$\boldsymbol{k}'$ scattering plane is not determined and the value of these PDDCSs with $q \neq 0$ must be zero [38]. The PDDCSs $(2\pi/\sigma)(\mathrm{d}\sigma_{22+}/\mathrm{d}\omega_t)$ is related to $\langle \sin 2\theta_r \cos 2\phi_r \rangle$, and it is obvious that the value of it is negative for a majority of all the scattering angles, which indicates the prominent preference of product alignment along the *y*-axis. It is interesting that four collision energies have a consistent polarization trend for $(2\pi/\sigma)(\mathrm{d}\sigma_{22+}/\mathrm{d}\omega_t)$. The strongest polarization of the product molecule are at about 30°, and the product displays a stronger polarization at E_{col} = 20 kcal/mol. The value of $(2\pi/\sigma)(\mathrm{d}\sigma_{21-}/\mathrm{d}\omega_t)$ is relative to $\langle -\sin 2\theta_r \cos 2\phi_r \rangle$, and the behavior of it changes as the collision energy increases. As is shown in Figure 4(d), at E_{col} = 0.5 kcal/mol, the value of $(2\pi/\sigma)(\mathrm{d}\sigma_{21-}/\mathrm{d}\omega_t)$ is clearly positive at about 165°, which denotes the product alignment is along the direction of vector $\boldsymbol{x}$–$\boldsymbol{z}$ at backward scattering angles. And far away this range, the product rotational angular momentum is more isotropic. However, at E_{col} = 2 and 8 kcal/mol, the product alignments are along the direction of vector $\boldsymbol{x}$+$\boldsymbol{z}$ at forward scattering angles and along the direction of vector $\boldsymbol{x}$–$\boldsymbol{z}$ at backward scattering angles, respectively. At E_{col} = 20 kcal/mol, the product H_2^+ is preferentially aligned along $\boldsymbol{x}$+$\boldsymbol{z}$ at forward scattering angles. It is notable that the result at 0.5 kcal/mol is quite different from others, especially for the PDDCSs. The behaviors of four PDDCSs change regularly with the increase of collision energy ranging from 2 to 20 kcal/mol. The exception of 0.5 kcal/mol is mainly due to the well effect and indirect reaction mechanism at low collision energies. The lower the collision energy is, the more remarkable the well effect is. Similar reaction mechanism was observed in ion-molecule reactions $H^+ + H_2$ and $D^+ + H_2$ [31,32] We are eagerly looking forward to the experimental studies of the stereodynamics for this reverse reaction, and a comparison can be conducted between theory and experiment.

3 Conclusions

In this paper, we employ the quasi-classical trajectory method to study the vector correlations between the product and reagent for reaction $H + NeH^+$ ($v = 0$, $j = 0$) at different collision energies. The distributions of $P(\theta_r)$, $P(\phi_r)$ and four PDDCSs are calculated. The results indicate that the rotational polarization of product H_2^+ have different characters at different collision energies. The title reaction is mainly dominated by direct reactive mechanism at both low and high collision energies. However, at low collision energies, indirect reactive mechanism plays a role. The products are mainly forward scattering at four collision energies, and the tendency of forward scattering increases quickly with the increasing of collision energy. The rotational angular momentum vectors $\boldsymbol{j}'$ of products is not only aligned, but also

oriented along *y*-axis, and a preference of changing from the "in-plane" mechanism to the "out-of-plane" mechanism emerges. In addition, the average rotational alignment parameter $\langle P_2(\boldsymbol{j}'\cdot\boldsymbol{k})\rangle$ of products is calculated, and the tendency of it agrees with the distribution of $P(\theta_r)$.

Thanks are due to Prof. Han for providing the potential energy surface. This work was supported by the National Natural Science Foundation of China (11105022) and the Fundamental Research Funds for the Central Universities (2012QN066, 2011QN155).

1 Chen M D, Han K L, Lou N Q. Theoretical study of stereodynamics for the reactions Cl+H_2/HD/D_2. J Chem Phys, 2003, 118: 4463–4470
2 Wang M L, Han K L, He G Z. Product rotational polarization in the photoinitiated bimolecular reaction A + BC→AB + C on attractive, mixed and repulsive surfaces. J Chem Phys, 1998, 109: 5446–5454
3 Wang M L, Han K L, He G Z. Product rotational polarization in the photoinitiated bimolecular reaction A + BC: Dependence on the character of the potencial energy surface for different mass combinations. J Phys Chem A, 1998, 102: 10204–10210
4 Yin S H, Guo M X, Li L, et al. Isotope effect of the stereodynamics in the reactions F + HCl→HF + Cl and F + DCl→DF + Cl. Chin Sci Bull, 2010, 55: 3868–3874
5 Song D, Liu K, Kong F A, et al. Neutral dissociation of methane in the ultra-fast laser pulse. Chin Sci Bull, 2008, 53: 1946–1950
6 Wang J F, Zhang C C, Wei D Q, et al. Docking and molecular dynamics studies on CYP2D6. Chin Sci Bull, 2010, 55: 1877–1880
7 Yang X M, Xie D Q, Zhang D H. Dynamical resonance in F + H_2 chemical reaction and rotational excitation effect. Chin Sci Bull, 2007, 52: 1009–1012
8 Fano U, Macek J H. Impact excitation and polarization of the emitted light. Rev Mod Phys, 1973, 45: 553–573
9 Case D E, Herschbach D R. Statistical theory of angular momentum polarization in chemical reactions. Mol Phys, 1975, 30: 1537–1564
10 Mcclelland G M, Herschbach D R. Symmetry properties of angular correlations for molecular collision complexes. J Phys Chem, 1979, 83: 1445–1454
11 Barnwell J D, Loeser J G, Herschbach D R. Angular correlations in chemical reactions: Statistical theory for four-vector correlations. J Phys Chem, 1983, 87: 2781–2786
12 Bilotta R M, Farrar J M. Low energy crossed beam study of the reaction H_2^+ + Ne → HNe^+ + H. J Chem Phys, 1981, 75: 1776–1783
13 Pijkeren D V, Boltjes E, Eck J V, et al. Vibrational-state-selected ion-molecule reaction cross sections at thermal energies. Chem Phys, 1984, 91: 293–304
14 Herman Z, Koyano I. Dynamics of chemical reactions of ions from beam scattering and state-selected studies. J Chem Soc Faraday Trans II, 1987, 83: 127–137
15 Zhang T, Qian X M, Tang X N, et al. A state-selected study of the H_2^+ (X, v^+ = 0–17, N^+ = 1) + Ne proton transfer reaction using the pulsed-field ionization-photoelectron-secondary ion coincidence scheme. J Chem Phys, 2003, 119: 10175
16 Kress J D, Walker R B, Hayes E F, et al. Quantum scattering studies of long-lived resonances for the reaction Ne + H_2^+→NeH^+ + H. J Chem Phys, 1994, 100: 2728–2742
17 Gilibert M, Blasco R M, González M, et al. Three dimensional quantum mechanical treatment of the reaction Ne + H_2 → NeH^+ + H. J Phys Chem A, 1997, 101: 6821–6823
18 Gilibert M, Giménez X, Huarte-Larrañaga F, et al. Accurate 3 dimensional quantum dynamical study of the Ne + H_2^+→NeH^+ + H reaction. J Chem Phys, 1999, 110: 6278–6287
19 Mayneris-Perxachs J, González M. Time-dependent quantum dynamics study of the Ne + H_2^+ (v = 0–9) and D_2^+ (v = 0–12) proton transfer reactions at thermal collision energies. J Phys Chem A, 2009, 113: 4105–4109
20 Pendergast P, Heck J M, Hayes E F, et al. Fit of the potential energy surface for the reaction Ne + H_2^+→NeH^+ + H using three different functional forms. J Chem Phys, 1993, 98: 4543–4547
21 Lü S J, Zhang P Y, Han K L, et al. Exact quantum scattering study of the Ne + H_2^+ reaction on a new *ab initio* potential energy surface. J Chem Phys, 2010, 132: 014303
22 Xiao J, Yang C L, Wang M S, et al. Collision energies effect on stereodynamics for Ne + H_2^+ → NeH^+ + H reaction. Chin Phys Lett, 2011, 28: 013101
23 Xiao J, Yang C L, Wang M S, et al. Isotopic effects on the stereodynamics for the Ne + H_2^+/HD^+/HT^+ reactions. Chem Phys, 2011, 379: 46–50
24 Davidson E R, Silver D W. Size consistency in the dilute helium gas electronic structure. Chem Phys Lett, 1977, 52: 403–406
25 Aguado A, Paniagua M. A new functional form to obtain analytical potentials of triatomic molecules. J Chem Phys, 1992, 96: 1265–1275
26 Yin S H, Guo M X, Li L, et al. Stereo-dynamics of the F + HCl →HF + Cl reaction. Int J Quant Chem, 2011, 111: 4400–4409
27 Yin S H, Guo M X, Gao H, et al. Quasi-classical trajectory study of the dynamics of the reaction F + DCl (v = 0, j = 0) →DF + Cl. Comput Theor Chem, 2011, 967: 19–25
28 Aoiz F J, Brouard M, Enriquez P A. Product rotational polarization in photon-initiated bimolecular reactions. J Chem Phys, 1996, 105: 4964–4982
29 Brouard M, Lambert H M, Rayner S P, et al. Product state resolved stereodynamics of the reaction H(^{2}S) + CO_2 OH($X^2\Pi_{3/2}$; v = 0, N = 5) CO($^1\Sigma^+$). Mol Phys, 1996, 89: 403–423
30 Han K L, He G Z, Lou N Q. Effect of location of energy barrier on the product alignment of reaction A + BC. J Chem Phys, 1996, 105: 8699–8704
31 Zhang C H, Zhang W Q, Chen M D. Theoretical studies of stereodynamics for the H^+ + H^2 (v = 0–3, j = 0) → H_2 + H^+ reaction. J Theor Comput Chem, 2009, 8: 403–415
32 Zhang W Q, Chen M D. Quasiclassical trajectory study of the stereodynamics for the reaction D^+ + H_2 (v=0, j = 0) → HD + H^+. J Theor Comput Chem, 2009, 8: 1131–1141
33 Zhang W Q, Cong S L, Zhang C H, et al. Theoretical study of dynamics for the abstraction reaction H′ + HBr (v = 0, j = 0) → H′H + Br. J Phys Chem A, 2009, 113: 4192–4197
34 Li X H, Wang M S, Pino I, et al. The stereodynamics of the two reactions: H + LiH^+ (v = 0, j = 0) → H_2 + Li^+ and H^+ + LiH (v = 0, j = 0) → H_2^+ + Li. Phys Chem Chem Phys, 2009, 11: 10438–10445
35 Lv J J, Liu X G, Liang J J, et al. Theoretical study of the stereodynamics of the H + HeH^+ (v = 0, j = 0) → H_2^+ + He reaction. Can J Phys, 2010, 88: 899–904
36 Li R J, Han K L, Li F E, et al. Rotational alignment of product molecules from the reactions Sr + CH_3Br, C_2H_5Br, n-C_3H_7Br, i-C_3H_7Br by means of PLIF. Chem Phys Lett, 1994, 220: 281–285
37 Han K L, Zhang L, Xu D L, et al. Experimental and theoretical studies of the reactions of excited calcium atoms with ethyl and *n*-propyl bromides. J Phys Chem A, 2001, 105: 2956–2960
38 Gómez-Carrasco S, Hernándezb M L, Alvariño J M. Quantum and quasiclassical state-selected O(^{1}D) + HF reaction dynamics and kinetics on a new MRCI ground singlet potential energy surface. Chem Phys Lett, 2007, 435: 188–193